Asian Journal of Chemistry; Vol. 24, No. 9 (2012), 3895-3898

ASIAN JOURNAL OF CHEMISTRY

www.asianjournalofchemistry.co.in

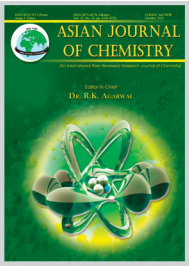

Theoretical Study of the Stereodynamics of the Reactions of Ne + $H_2^+ \rightarrow NeH^+ + H$ and Ne + $D_2^+ \rightarrow NeD^+ + D$

YULIANG WANG*, LIANGSHENG QU, YANLAN JIANG and JUNA CHEN

Department of Basic Sciences, Naval Aeronautical and Astronautical University, Yantai 264001, P.R. China

*Corresponding author: E-mail: yarmiay@163.com

(*Received*: 10 October 2011; *Accepted*: 18 April 2012) AJC-11264

Based on the adiabatic potential energy surface of the ground state l^2A' constructed by Lv *et al*. The probabilities of the reactions Ne + $H(D)_2^+ \rightarrow NeH(D)^+ + H(D)$ for $J = 0$ have been calculated by the quasiclassical trajectory method. Comparing the dynamics of Ne + $D_2^+ \rightarrow NeD^+ + D$ with Ne + $H_2^+ \rightarrow NeH^+ + H$, the four generalized polarization dependent differential cross-sections (PDDCSs) $(2\pi/\sigma)(d\sigma_{00}/d\omega_t)$, $(2\pi/\sigma)(d\sigma_{20}/d\omega_t)$, $(2\pi/\sigma)(d\sigma_{22+}/d\omega_t)$, $(2\pi/\sigma)(d\sigma_{21-}/d\omega_t)$ have been calculated in the centre of mass frame, respectively. The $P(\theta_r)$, $P(\phi_r)$ and $P(\theta_r, \phi_r)$ distributions, the k-k'-j' correlation and the angular distribution of product rotational vectors are presented in the form of polar plots. A pronounced isotope effect on the product polarization is also revealed. This effect may be derived from the different mass factor or the effective potential well depth in the two reactions.

Key Words: Isotope effect, Ne+H(D)$_2^+$ reactions, Quasiclassical trajectory, Vector relation.

INTRODUCTION

In recent decade, the endothermic atom-molecule ion reaction has been studied, theoretically and experimentally[1-11]. For the experiments, Pijkeren *et al*.[2] measured the relative energy dependent cross sections for H_2^+ (v = 0-8) using the photoelectron-secondary ion coincidence (PESICO) technique. Relative cross sections for v = 0-4 were determined as a function of translational energies in a threshold electron secondary ion coincidence (TESICO) experiment[3]. Zhang *et al*.[4] and Dressler *et al*.[5] used the pulsed field ionization photoelectron secondary ion coincidence (PFI-PESICO) scheme to measure the integral cross sections for the two lowest reactant vibrational levels v = 0 and 1 at high signal-to-noise ratio through ion preparation using intense auto-ionization resonances. Sharp threshold onsets were observed, suggesting the importance of long-lived intermediates or resonances. And the endothermicity is 0.54 and 0.27 eV for reactant vibrational levels v = 0 and 1, respectively. Considering theoretical aspect, many groups have constructed the potential energy surface (PES)[8-12] using different methods and many dynamics calculations have also been done. Based on the bending corrected rotating linear model, Kress *et al*.[13] determined the state-to-state reaction probabilities for total angular momentum $J = 0$, finding the effectivity of vibrational excitation in promoting reactivity and the extremely structured shape of the reaction probability as a function of energy[14]. Gilibert and coworkers[15,16] calculated the state-selected integral cross sections using the coupled-states approximation (CSA), indicating the summation over J enhances the peak structure. Recently, Mayneris *et al*.[17] carried out a time-dependent real wave packet (RWP) quantum study for Ne + $H_2^+ \rightarrow NeH^+ + H$ and Ne + $D_2^+ \rightarrow NeD^+ + D$ to determine the reaction probabilities and cross sections, presenting many resonances in Ne + H_2^+ proton transfer probabilities and oscillatory behaviour of the cross sections. Utilizing the same method, they also studied the influence of vibrational excitation of H_2^+ and D_2^+ on the dynamics at thermal collision energies[2,5,18,19]. In addition, especially due to the abundance of D (deuterium) in the nature, many researches related to the isotopic reactions systems have been done, which also revealed some pronounced effects of isotope to the stereodynamics[19,20]. Toshiyuki *et al*.[21] calculated for the F + $H(D)_2$ using three-dimensional quantum scattering method with an emphasis on the threshold behaviour of the reaction probabilities and the results show that the Van der Waals potential plays an important role in reaction dynamics. Aoiz *et al*.[22] carried out the calculations for the reactions F + $H(D)_2$ using both QM and QCT methods, the intermolecular isotope effect, *i.e.*, the ratio between the cross sections of the CI + n - $H(D)_2$ reacions, Γ_{inter} (CI + n-H_2/CI + n-D_2) , predicted by QM calculations on the BW2 surface is notably larger than that obtained experimentally. More recently, using highly correlated complete active space self-consistent field and multireference configuration interaction wave functions with a basis set of aug-cc-pV5Z,

Lv *et al.*[18] presented a new PES for the ground state l^2A' and performed quantum reactive scattering dynamics calculation taking the Coriolis coupling (CC) effect into account. The results are found to be in good agreement with the experimental measurements obtained by Zhang *et al.*[4].

As mentioned above, due to its importance, the reaction of Ne + H_2^+ and its isotopic variants have attracted enormous attention. It is quite necessary to study their vector properties to understand the dynamics of the title reactions fully, which can provide the valuable information about chemical reaction stereo-dynamics[17,23]. As we know, the isotope effect plays significant roles in the deduction of chemical reaction mechanics. In the present work, to shed more light on the state-to-state dynamics of these ion-molecule reactions, based on the global PES of the l^2A' adiabatic electronic state[18], we present a QCT study for vector properties to find how tiny difference of the characteristics of the two systems affect the stereodynamics between the reaction Ne + H_2^+ and Ne + D_2^+.

COMPUTING SCHEME

In our calculation, the PES we used was constructed by Lv *et al.*[18], who fitted a set of accurate *ab initio* points to two- and three-body polynomial expansion in the Aguado-Paniagua functional form[24]. The detailed functional form and deduction process can be found[18].

The calculation method of QCT is the same as that of Refs[19,20,25]. The classical Hamilton's equations are integrated numerically for motion in three dimensions. In present work, the trajectory is initiated in the $v = 0$ and $j = 0$ levels and the collision energy is chosen as 1.2 eV for the title reactions. In the calculation, a batch of 20000 trajectories is run for each reaction and the integration step size is chosen to be 0.1 fs, which can guarantee the conservation of the total energy and total angular momentum.

Later, Han *et al.*[23] developed the stereodynamical QCT computational method and the product rotational polarization of many chemical reactions[18-20,25] has been well studied by this method. In the center-of-mass (CM) frame, the reagent relative velocity vector k is parallel to the z axis while the y axis is perpendicular to the x-z plane containing the initial and final relative velocity vectors, k and k'. θ_t is the so-called scattering angle between the reagent relative velocity and the product relative velocity, while θ_r and ϕ_r refer to the coordinates of the unit vectors k' and j' along the directions of the product relative velocity and rotational angular momentum vectors.

The polar angle distribution $P(\theta_r)$ describing the k-j' correlation which can be expanded into a series of Legendre polynomials is defined as:

$$P(\theta_r) = \frac{1}{2}\sum_k [k] a_0^{(k)} P_k(\cos\theta_r) \quad (1)$$

The expanding coefficients $a_0^{(k)}$ called polarization parameters are given by:

$$a_0^{(k)} = \int_0^{\pi} P(\theta_r) P_k(\cos\theta_r) \sin\theta_r d\theta_r = \langle P_k(\cos\theta_r) \rangle \quad (2)$$

The dihedral angle distribution function $P(\phi_r)$ describing k-k'-j' correlation can be expanded in Fourier series as:

$$P(\phi_r) = \frac{1}{2\pi}(1 + \sum_{even,n\geq 2} a_n \cos n\phi_r + \sum_{odd,n\geq 1} a_n b_n \sin n\phi_r) \quad (3)$$

where,

$$a_n = 2\langle \cos n\phi_r \rangle \quad (4)$$

$$b_n = 2\langle \sin n\phi_r \rangle \quad (5)$$

The joint probability density function of angles θ_r and ϕ_r, which define the direction of j', the space distribution of the product's rotation angular momentum can be written as:

$$P(\theta_r, \phi_r) = \frac{1}{4\pi}\sum_{kq} [k] a_q^k C_{kq}(\theta_r \phi_r)^*$$
$$= \frac{1}{4\pi}\sum_k \sum_{q\geq 0} [a_{q\pm}^k \cos\phi_r - a_{q\mp}^k \sin q\phi_r] C_{kq}(\theta,0) \quad (6)$$

In this work, $P(\theta_r)$, $P(\phi_r)$ and $P(\theta_r, \phi_r)$ are expanded up to k = 18, n = 24, k = 7, which shows a good convergence.

The fully correlated CM angular distribution which can be represented by a set of generalized polarization-dependent differential cross-sections (PDDCSs) is written as:

$$P(\omega_t, \omega_r) = \sum_{kq} \frac{[k]}{4\pi} \frac{1}{\sigma} \frac{d\sigma_{kq}}{d\omega_t} C_{kq}(\theta_r, \theta_r)^* \quad (7)$$

where $(1/\sigma)(d\sigma_{kq}/d\omega_t)$ is a generalized polarization dependent differential cross-s-ection (PDDCS). Many photo-initiated bimolecular reaction experments are sensitive to only those polarization moments with k = 0 and k = 2. In the present work, $(2\pi/\sigma)(d\sigma_{00}/d\omega_t)$, $(2\pi/\sigma)(d\sigma_{20}/d\omega_t)$, $(2\pi/\sigma)(d\sigma_{22+}/d\omega_t)$ and $(2\pi/\sigma)(d\sigma_{21-}/d\omega_t)$ are calculated. In the above calculations, PDDCSs are expanded up to $k_1 = 7$, which is sufficient for good convergence.

The distribution of the angular momentum j' of the product molecule is described by a function $f(\theta_r)$, where θ_r is the angle between j' and k. $f(\theta_r)$ can be represented by the Legendre polynomial.

$$f(\theta_r) = \Sigma a_l P_l(\cos\theta_r) \quad (8)$$

where, l = 2 indicates the product rotational orientation defined as:

$$\langle P_2(j'.k) \rangle = \frac{1}{2}\langle 3\cos^2\theta_r - 1 \rangle \quad (9)$$

RESULTS AND DISCUSSION

Fig. 1 shows the comparison of the reaction probabilities between Ne + H_2^+ and Ne + D_2^+. As shown in this figure, the tendency of the reaction probabilities of Ne + H_2^+ and Ne + D_2^+ approximately agree with each other in the whole collision energy range, it is clear that the reaction probabilities become increasingly higher with the increase of the collision energy.

In order to make further investigation for the dynamics of the reactions and also to reveal the isotope effect of the title reactions, the vector properties have also been studied. The polarization dependent generalized differential cross section (PDDCS) which can describe the k-k'-j' correlation and the scattering direction of the product has been calculated and the results are shown in Fig. 2 with the corresponding collision energy 1.2 eV, respectively.

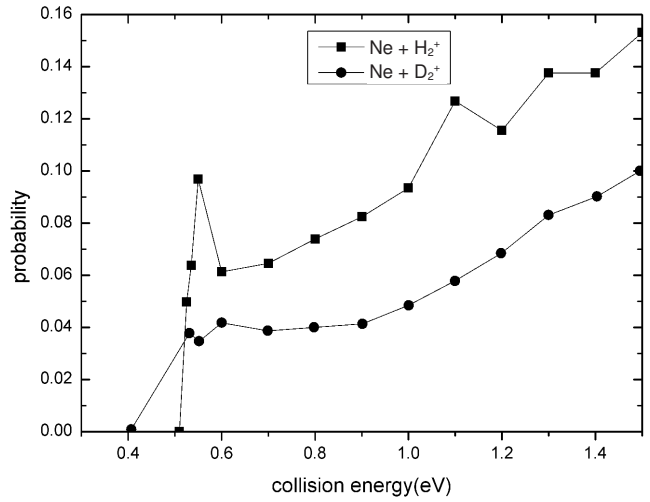

Fig. 1. A comparison of the reaction probabilities between Ne + H_2^+ and Ne + H_2^+

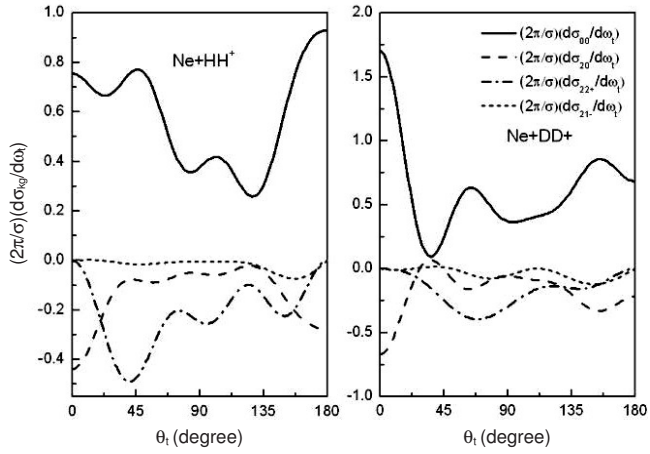

Fig. 2. A comparison of the polarization dependent generalized differential cross section between the Ne + H_2^+ and Ne + D_2^+ at the collision energy of 1.2 eV

The PDDCS $(2\pi/\sigma)(d\sigma_{00}/d\omega_t)$ is simply the (k, k') differential cross section (DCS), which describes the angluar distribution of the product molecule ion. It is obvious that the NeH^+ product is slightly backward scattering, while the NeH^+ product is almost forward scattering. The PDDCS $(2\pi/\sigma)(d\sigma_{20}/d\omega_t)$ is the expectation value of the second Legendre moment $\langle P_2(\cos\theta_r)\rangle$ and the trend of it is indistinctively opposite to that of $(2\pi/\sigma)(d\sigma_{00}/d\omega_t)$, indicating that j' is strongly aligned perpendicular to k. It is obvious that the PDDCSs with $q \neq 0$ are zero at the extremities of forward and backward scattering. The behaviour of PDDCSs with $q \neq 0$ at the scattering away from extreme forward and backward direction is more interesting[26]. It provides information on the ϕ_r dihedral angel distribution. The values are nonzero at scattering angles away from $\theta_t = 0$ and π, which indicates the $P(\theta_r, \phi_r)$ distribution is not isotropic for backward scattering products. The PDDCS $(2\pi/\sigma)(d\sigma_{22+}/d\omega_t)$ is related to $\langle \sin^2\theta_r \cos 2\phi_r \rangle$. As can be seen from Fig. 2, for the title reactions, the values of $(2\pi/\sigma)(d\sigma_{22+}/d\omega_t)$ are negative for all scattering angles, which indicating the remarkable preference of product alignment along the y-axis, the strongest polarization of the products of the two reactions are at about 45º and 65º. The value of $(2\pi/\sigma)(d\sigma_{21+}/d\omega_t)$ is related to $\langle -\sin 2\theta_r \cos\phi_r \rangle$ and it can been seen, for the collision energy 1.2 eV, $(2\pi/\sigma)(d\sigma_{21-}/d\omega_t)$ are nearly zero indicating the product alignment is isotropic at the wide range of scattering angles.

In order to get a better graphical representation of the polarization of the products from the title reactions, we have plotted $P(\theta_r)$ and $P(\phi_r)$ distributions at the same collision energy 1.2 eV in Figs. 3 and 4, respectively. The distribution describes the k-j' correlation, which is plotted in Fig. 3. It is clearly that the $P(\theta_r)$ distributions peak at θ_r angles, which close to $\pi/2$ and are symmetric with respect to $\pi/2$, which shows that the product rotational angular momentum vector is strongly aligned along the direction at right angle to the relative velocity direction. As shown in the figure, the peak of $P(\theta_r)$ distributions for the reaction Ne + D_2^+ is higher than that of Ne + H_2^+, which indicates that the degree of alignment of NeD^+ is stronger than that of NeH^+. On the condition of adiabatic approximation, the influence of isotopic substitution on the PES is not considered here. In our calculation, the PES of the two reactions is same, so we consider that the difference of the $P(\theta_r)$ distributions is probably attributed to the difference of the mass factor between the two reactions. The $P(\phi_r)$ distributions are shown in Fig. 4. It describes k-k'-j' correlations. $P(\phi_r)$ distributions have no sharp peaks at $\pi/2$ and $3\pi/2$ for Ne + D_2^+ reaction, while there are two peaks in $\pi/2$ and $3\pi/2$ for Ne + H_2^+ reaction, which shows that the rotational angular momentum vectors of NeH^+ are mainly aligned along the y-axis in the CM frame. The peak at $3\pi/2$ is stronger than that at $\pi/2$, indicating that the product rotational angular momentum vector is not only aligned, but also oriented along the negative y-axis. The orientation degree of the products NeH^+ is stronger than that of NeD^+. According to the work of Lip *et al.*[27], the difference may be due to the different harmonic zero point energy (ZPE) of the reactant ions NeH^+ and NeD^+, which induces the different effective potential well depth of the two reactions. The effect potential well of the Ne + H_2^+ reaction is shallower than that of the Ne + D_2^+ reaction which leads to the product NeH^+ orienting more strongly than NeD^+.

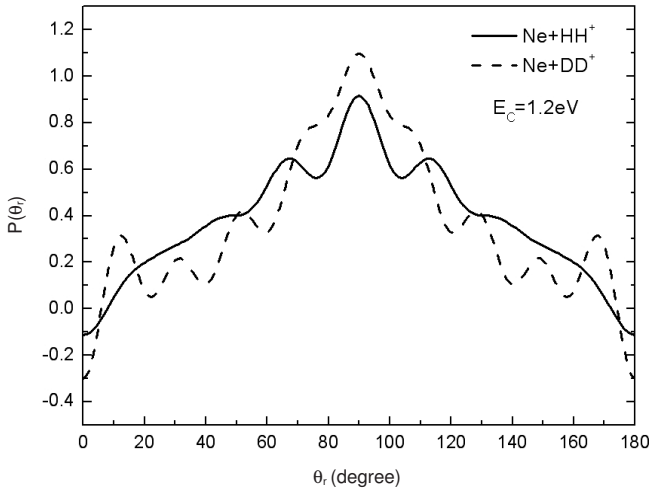

Fig. 3. Distribution of $P(\theta_r)$, reflecting the k-j' correlation at the collision energy of 1.2 eV

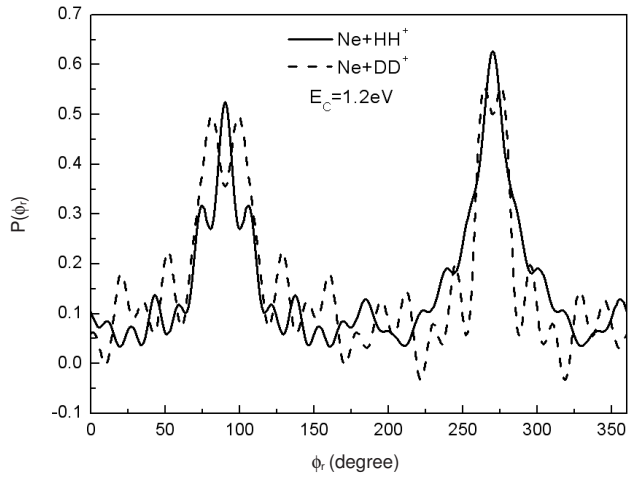

Fig. 4. Dihedral angle distribution of $P(\phi_r)$ for title reactions with respect to the k,k' plane

In order to validate more information of the angular momentum polarization, we also plot the angular momentum polarization in the form of polar plots in θ_r and ϕ_f averaged over all scattering angles in Fig. 5. The distributions of $P(\theta_r, \phi_r)$ are in good accordance with the distributions of $P(\theta_r)$ and $P(\phi_r)$ of the NeH^+ products and NeD^+ products at the collision of 1.2 eV. These two reactions belong to heavy-light-light (HLL) mass combination, which leads to the fact that the product orbital angular momentum is large and the reactant orbital angular momentum has less influence on the product rotational alignment, which is also consistent with the previous prediction[23].

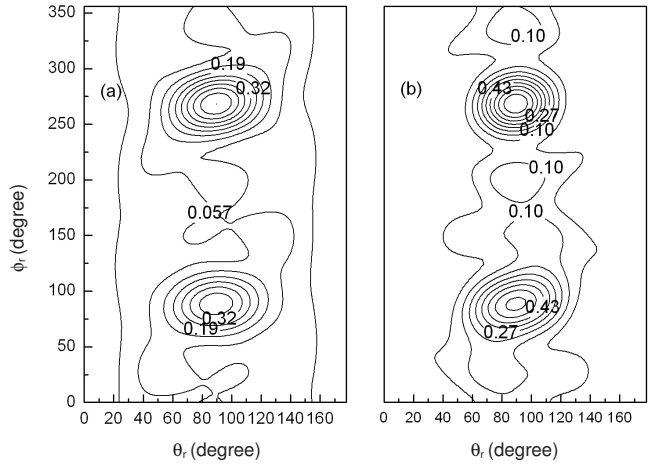

Fig. 5. Polar plots of $P(\theta_r, \phi_r)$ distribution for Ne + H_2^+ and Ne + D_2^+ at the collision energy of 1.2 eV over averaged over all scattering angles

Conclusion

This paper has presented a QCT calculation for the dynamics of the reactions $Ne+H(D)_2^+$ based on the l^2A' PES at the same collision energy of 1.2 eV. The results of reaction probability of $Ne+H(D)_2^+ \rightarrow NeH(D)^+ + D$ reactions have been found to be consistent with each other. In addition, the stereo dynamics of the title reactions have also been studied. The calculated PDDCSs indicate that the product NeH^+ is mainly backward scattering and NeD^+ is mainly forward scattering. According to investigating the vector properties of the title reactions, a pronounced isotope effect is revealed, which comes from the difference of the mass factor and the different effective potential well depth of the two reactions.

ACKNOWLEDGEMENTS

This study was supported by the State Key Laboratory of Molecular Reaction Dynamics, Dalian Institute of Chemical Physics, Chinese Academy of Sciences. Many thanks to Shuangjiang Lv for providing the potential energy surface and Prof. Keli Han for providing the code.

REFERENCES

1. R.M. Bilotta and J.M. Farrar, *J. Chem. Phys*., **75**, 1776 (1981).
2. D. Van Pijkeren, E. Boltjes, J.V. Eck and A. Niehaus, *J. Chem. Phys.*, **91**, 293 (1984).
3. Z. Herman and I. Koyano, *J. Chem. Soc., Farad. Trans II*, **83**, 127 (1987).
4. T. Zhang, X.-M. Qian, X.N. Tang, C.Y. Ng, Y. Chiu, D.J. Levandier, J.S. Miller and R.A. Dressler, *J. Chem. Phys*., **119**, 10175 (2003).
5. R.A. Dressler, Y. Chiu, D.J. Levandier, X.N. Tang, Y. Hou, C. Chang, C. Houchins, H. Xu and C.Y. Ng, *J. Chem. Phys*., **125**, 132306 (2006).
6. L. González-Sánchez, S. Gómez-Carrasco and A. Aguado, *J. Chem. Phys*., **121**, 309 (2004).
7. S. Gómez-Carrasco, O. Roncero and L. González-Sánchez, *J. Chem. Phys*., **123**, 114310 (2005).
8. P.J. Kuntz and A.C. Roach, *J. Chem. Soc., Faraday Trans. 2,* **68**, 259 (1972).
9. M. González, R.M. Blasco, X. Giménez and A. Aguilar, *J. Chem. Phys*., **209**, 355 (1996).
10. F. Huarte-Larranaga, X. Giménez, J.M. Lucas, A. Aguilar and J.-M. Launay, *J. Phys. Chem. A*, **104**, 10227 (2000).
11. P. Pendergast, J.M. Heck, E.F. Hayes and R. Jaquet, *J. Chem. Phys*., **98**, 4543 (1993).
12. J. Urban, R. Jaquet and V. Staemmler, *Int. J. Quantum Chem*., **38**, 339 (1990).
13. J.D. Kress, R.B. Walker, E.F. Hayes and P. Pendergast, *J. Chem. Phys*., **100**, 2728 (1994).
14. F. Huarte-Larrañaga, X. Giménez, J.M. Lucas, A. Aguilar and J.-M. Launay, *Phys. Chem. Chem. Phys*., **1**, 1125 (1999).
15. M. Gilibert, R.M. Blasco, M. González, X. Giménez, A. Aguilar, I. Last and M. Baer, *J. Phys. Chem. A*, **101**, 6821 (1997).
16. M. Gilibert, X. Giménez, F. Huarte-Larrañaga, M. González, A. Aguilar, I. Last and M. Baer, *J. Chem. Phys*., **110**, 6278 (1999).
17. J. Mayneris, J.D. Sierra and M. González, *J. Chem. Phys*., **128**, 194307 (2008).
18. S.J. Lv, P.Y. Zhang, K.L. Han and G.Z. He, *J. Chem. Phys*., **132**, 014303 (2010).
19. M.D. Chen, K.L. Han and N.Q. Lou, *J. Chem. Phys*., **118**, 4463 (2003).
20. M.D. Chen, K.L. Han and N.Q. Lou, *Chem. Phys. Lett.,* **357**, 483 (2002).
21. Toshiyuki, Takayanagi, Yuzuru and Kurosaki, *Chem. Phys.Lett*., **286**, 35 (1998).
22. F.J. Aoiz, L. Bañares, J.F. Castillo and M. Menéndez, *J. Chem. Phys*., **115**, 5 (2001).
23. K.L. Han, G.Z. He and N.Q. Lou, *J. Chem. Phys*., **105**, 8699 (1996).
24. A. Aguado and M. Paniagua, *J. Chem. Phys*., **96**, 1265 (1992).
25. M.L. Wang, K.L. Han and G.Z. He, *J. Chem. Phys*., **109**, 5446 (1998).
26. F.J. Aoiz, M. Brouard and P.A. Enriquez, *J. Chem. Phys*., **105**, 4964 (1996).
27. S.Y. Lin, K.L. Han and J.Z.H. Zhang, *Chem. Phys. Lett*., **324**, 122 (2000).